

VALIDATING THE NEUTROSOPHIC APPROACH OF MRI DENOISING BASED ON STRUCTURAL SIMILARITY

J. Mohan^{}, V. Krishnaveni^{*}, Yanhui Guo[#]*

^{}Department of ECE, PSG College of Technology, Coimbatore, Tamilnadu, India-641004.*

Email: jaimohan12@gmail.com; vk@ece.psgtech.ac.in

[#]Department of Radiology, University of Michigan, Ann Arbor, MI 48109, USA.

Email: yanhuig@med.umich.edu

Keywords: Magnetic Resonance Image, Denoising, Neutrosophic Set, SSIM, QILV, PSNR.

Abstract

This paper focuses on validating the proposed Neutrosophic Set (NS) approach of Magnetic Resonance Image (MRI) denoising based on structural similarity such as Structural Similarity Index (SSIM) and Quality Index based on Local Variance (QILV). The Neutrosophic Set approach of median filter is used to reduce the Rician noise in MR image. The experiments have conducted on real MR image with Rician noise added. The visual and the diagnostic quality of the denoised image is well preserved. The performance of this filter is compared with median filter and non local mean filter (NLM).

1 Introduction

Magnetic resonance imaging (MRI) is the most powerful imaging technique [22] developed to study the structural features and the functional characteristics of the internal body parts. The diagnostic and visual quality of the MR images are affected by the noise added while acquisition. This is problematic for further tasks such as segmentation of important features; classification of images for computer aided diagnostics, three dimensional image reconstruction and image registration. Therefore, denoising should be performed to improve the image quality for more accurate diagnosis.

The MR image is commonly reconstructed by computing the inverse Discrete Fourier Transform of the raw data. The signal component of the measurement is present in both real and imaginary channels. Each of the orthogonal channels is affected by additive white Gaussian noise. The noise in the reconstructed complex valued data is thus complex white Gaussian noise. Most commonly, the magnitude of the reconstructed MRI image is used for visual inspection and for automatic computer analysis. Since the magnitude of the MRI signal is the square root of the sum of the squares of two independent Gaussian variables, it follows Rician distribution [8]. The Rician noise is signal dependent and is therefore difficult to separate from the signal.

Numerous approaches of denoising MR images have been

proposed including approaches based on anisotropic diffusion [7,10,19,20,26], the wavelet transform [2,6,15,16,17,25], bilateral and trilateral filtering [9,23,24], the non-local means algorithm [3-5,11-13] in the literatures. This paper is an extended work of [14]. The Neutrosophic Set approach of MRI denoising is validated in terms of structural similarity (SSIM) [21] index and quality index based on local variance (QILV) [1]. As already mentioned in [1, 21], peak signal to noise ratio (PSNR) is not the reliable quality metric with respect to human visual system (HVS). SSIM is an objective quality measure based on the structural content of the image that engulfs the properties of HVS. Medical images contain delicate structural features that contribute more to the diagnosis. QILV will provide the statistical similarity between the denoised and the original image.

2 Neutrosophic MRI denoising

Neutrosophy, a branch of philosophy introduced in [18] as a generalization of dialectics, studies the origin, nature and scope of neutralities, as well as their interactions with different ideational spectra. Neutrosophy theory considers proposition, theory, event, concept or entity, $\langle A \rangle$ is in relation to its opposite $\langle \text{Anti-}A \rangle$ and the $\langle \text{Neut-}A \rangle$ which is neither $\langle A \rangle$ nor $\langle \text{Anti-}A \rangle$. The neutrosophy is the basis of the neutrosophic logic, neutrosophic probability, and neutrosophic set and neutrosophic statistics [18]. In neutrosophic set, the indeterminacy is quantified explicitly and the truth-membership, indeterminacy-membership and falsity-membership are independent. The neutrosophic set is a general formal frame work which generalizes the concept of the classic set, fuzzy set, interval valued fuzzy set, intuitionistic fuzzy set, and interval valued intuitionistic fuzzy set, paraconsistent set, dialetheist set, paradoxist set and tautological set [18]. The neutrosophic set had been applied into image processing such as denoising [27], segmentation [28, 29]. The definition of a neutrosophic set and its properties are described briefly.

2.1 Neutrophic Set

Definition 1 (Neutrosophic Set). Let U be a Universe of discourse and a neutrosophic set A is included in U . An element x in set A is noted as $x(T, I, F)$. T, I, F are real

standard and non standard sets of $]^{-0,1^+}$ with $\sup T = t_sup, \inf T = t_inf, \sup I = i_sup, \inf I = i_inf, \sup F = f_sup, \inf F = f_inf$ and $n_sup = t_sup + i_sup + f_sup, n_inf = t_inf + i_inf + f_inf$.

T, I and F are called the neutrosophic components. The element $x(T, I, F)$ belongs to A in the following way. It is $t\%$ true in the set, $i\%$ indeterminate in the set, and $f\%$ false in the set, where t varies in T , i varies in I and f varies in F .

2.2 Transform the image into neutrosophic set

Definition 2 (Neutrosophic image). Let U be a Universe of discourse and W is a set of U , which is composed by bright pixels. A neutrosophic image P_{NS} is characterized by three membership sets T, I, F . a pixel P in the image is described as $P(T, I, F)$ and belongs to W in the following way: It is t true in the set, i indeterminate in the set, and f false in the set, where t varies in T , i varies in I and f varies in F . Then the pixel $P(i, j)$ in the image domain is transformed into the neutrosophic set domain $P_{NS}(i, j) = \{T(i, j), I(i, j), F(i, j)\}$. $T(i, j), I(i, j)$ and $F(i, j)$ are the probabilities belong to white pixels set, indeterminate set and non white pixels set respectively, which are defined as:

$$T(i, j) = \frac{\bar{g}(i, j) - \bar{g}_{\min}}{\bar{g}_{\max} - \bar{g}_{\min}} \quad (1)$$

$$\bar{g}(i, j) = \frac{1}{w \times w} \sum_{m=i-w/2}^{i+w/2} \sum_{n=j-w/2}^{j+w/2} g(m, n) \quad (2)$$

$$I(i, j) = \frac{\delta(i, j) - \delta_{\min}}{\delta_{\max} - \delta_{\min}} \quad (3)$$

$$\delta(i, j) = \text{abs}(g(i, j) - \bar{g}(i, j)) \quad (4)$$

$$F(i, j) = 1 - T(i, j) \quad (5)$$

where $\bar{g}(i, j)$ is the local mean value of the pixels of the window. $\delta(i, j)$ is the absolute value of difference between intensity $g(i, j)$ and its local mean value $\bar{g}(i, j)$.

2.3 Neutrosophic image entropy

For a gray image, the entropy is utilized to evaluate the distribution of the gray levels. If the entropy is the maximum, the intensities have equal probability. If the entropy is small, the intensity distribution is non-uniform.

Definition 3 (Neutrosophic image entropy). Neutrosophic entropy of an image is defined as the summation of the entropies of three subsets T, I and F :

$$En_{NS} = En_T + En_I + En_F \quad (6)$$

$$En_T = - \sum_{i=\min\{T\}}^{\max\{T\}} p_T(i) \ln p_T(i) \quad (7)$$

$$En_I = - \sum_{i=\min\{I\}}^{\max\{I\}} p_I(i) \ln p_I(i) \quad (8)$$

$$En_F = - \sum_{i=\min\{F\}}^{\max\{F\}} p_F(i) \ln p_F(i) \quad (9)$$

where En_T, En_I and En_F are the entropies of sets T, I and F respectively. $p_T(i), p_I(i)$ and $p_F(i)$ are the probabilities of elements in T, I and F respectively, whose values equal to i .

2.4 γ - median filtering operation

The values of $I(i, j)$ is employed to measure the indeterminate degree of element $P_{NS}(i, j)$. To make the set I correlated with T and F , the changes in T and F influence the distribution of element in I and vary the entropy of I .

Definition 4 (γ - median filtering operation). A γ - median filtering operation for $P_{NS}, \hat{P}_{NS}(\gamma)$, is defined as:

$$\hat{P}_{NS}(\gamma) = P(\hat{T}(\gamma), \hat{I}(\gamma), \hat{F}(\gamma)) \quad (10)$$

$$\hat{T}(\gamma) = \begin{cases} T & I < \gamma \\ \hat{T}_\gamma & I \geq \gamma \end{cases} \quad (11)$$

$$\hat{T}_\gamma(i, j) = \text{median}_{(m,n) \in S_{i,j}} \{T(m, n)\} \quad (12)$$

$$\hat{F}(\gamma) = \begin{cases} F & I < \gamma \\ \hat{F}_\gamma & I \geq \gamma \end{cases} \quad (13)$$

$$\hat{F}_\gamma(i, j) = \text{median}_{(m,n) \in S_{i,j}} \{F(m, n)\} \quad (14)$$

$$\hat{I}_\gamma(i, j) = \frac{\delta_{\hat{T}}(i, j) - \delta_{\hat{T}_{\min}}}{\delta_{\hat{T}_{\max}} - \delta_{\hat{T}_{\min}}} \quad (15)$$

$$\delta_{\hat{T}}(i, j) = \text{abs}(\hat{T}(i, j) - \bar{\hat{T}}(i, j)) \quad (16)$$

$$\hat{T}(i, j) = \frac{1}{w \times w} \sum_{m=i-w/2}^{i+w/2} \sum_{n=j-w/2}^{j+w/2} \hat{T}(m, n) \quad (17)$$

where $\delta_{\hat{T}}(i, j)$ is the absolute value of difference between intensity $\hat{T}(i, j)$ and its local mean value $\hat{\bar{T}}(i, j)$ at (i, j) after γ -median filtering operation.

The summary of neutrosophic set approach of MRI denoising is described as below (see figure 1):

- Step 1: Transform the image into NS domain;
Step 2: Use γ -median filtering operation on the true subset T to obtain \hat{T}_{γ} ;
Step 3: Compute the entropy of the indeterminate subset $\hat{I}_{\gamma}, En_{\hat{I}_{\gamma}}(i)$;
Step 4: if $\frac{En_{\hat{I}_{\gamma}}(i+1) - En_{\hat{I}_{\gamma}}(i)}{En_{\hat{I}_{\gamma}}(i)} < \delta$, go to Step 5;
Else $T = \hat{T}_{\gamma}$, go to Step 2;
Step 5: Transform subset \hat{T}_{γ} from the neutrosophic domain into the gray level domain.

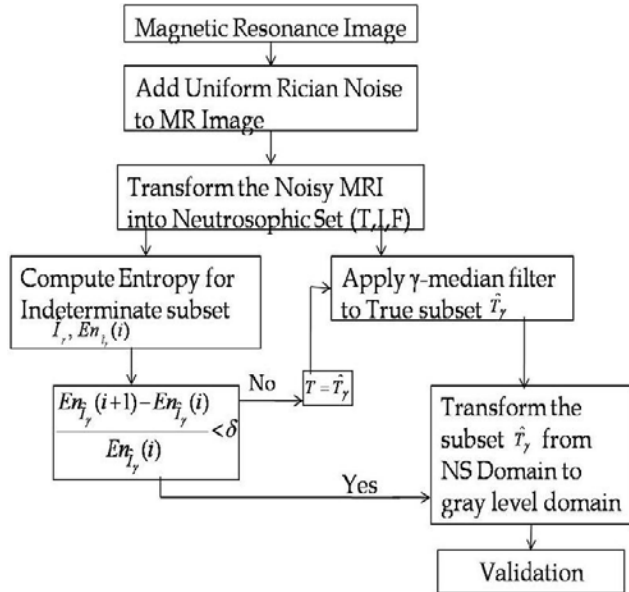


Figure 1: Neutrosophic Set approach of MRI denoising

3 Results and Validation

Two brain MR images of 5th slice, T2 Axial with repetition/echo time (TR/TE) 9000/87 ms and T1 Sagittal with TR/TE 552/17 ms which are obtained using SIEMENS 1.5 T MRI scanner for a 2 years old male child are considered for the experiments. This method is compared with median filter and Non Local Mean (NLM) filter proposed by Buades *et al* [3]. The results of the different denoising filters on a brain MRI corrupted with Rician noise is shown in Figure 2.

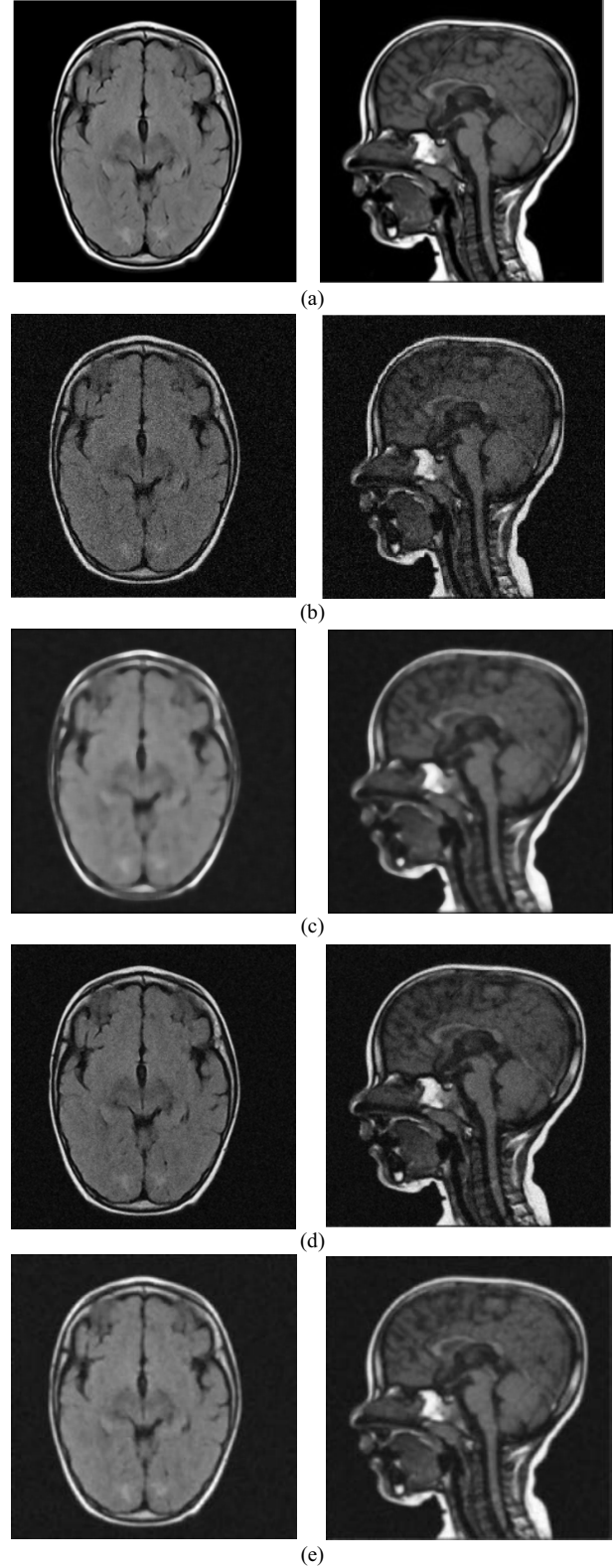


Figure 2: Results of different denoising filters on a brain MRI corrupted with Rician noise of standard deviation $\sigma_n=15$. T2 Axial (left) and T1 Sagittal (right) slices. From top to bottom: (a) the original image, (b) the noise corrupted image, and the results of (c) median filter, (d) the non local mean filter and (e) the neutrosophic set filter.

The performance of the denoising algorithm is measured by using the peak-signal-to-noise ratio (PSNR), the Structural Similarity (SSIM) index] and the Quality Index based on Local Variance (QILV). The PSNR will give the pixel by pixel similarity. The peak signal to noise ratio in decibel (dB) is measured using the following formula:

$$PSNR = -10 \log \left[\frac{\sum_{i=0}^{H-1} \sum_{j=0}^{W-1} (I(i, j) - I_d(i, j))^2}{H \times W \times 255^2} \right] \quad (18)$$

where $I(i, j)$ and $I_d(i, j)$ represent the intensities of pixels (i, j) in the original image and denoised image respectively. The higher the PSNR, the better the denoising algorithm is.

SSIM and QILV give the measure of the structural similarity between the original and the denoised images and are in the range of 0 to 1. The SSIM works as follows: Let x and y be two non negative images, where x has perfect quality. Then, the SSIM can serve as a quantitative measure of the similarity of the second image. The system separates the task of similarity measurement into three comparisons: luminance, contrast and structure. It can be defined as

$$SSIM(x, y) = \frac{(2\mu_x\mu_y + C_1)(2\sigma_{xy} + C_2)}{(\mu_x^2 + \mu_y^2 + C_1)(\sigma_x^2 + \sigma_y^2 + C_2)} \quad (19)$$

where μ_x and μ_y are the estimated mean intensity and σ_x and σ_y are the standard deviations respectively. σ_{xy} can be estimated as

$$\sigma_{xy} = \frac{1}{N-1} \sum_{i=1}^N (x_i - \mu_x)(y_i - \mu_y) \quad (20)$$

C_1 and C_2 in eqn. 19 are constants and the values are given as $C_1 = (K_1L)^2$ and $C_2 = (K_2L)^2$ where $K_1, K_2 \ll 1$ is a small constant and L is the dynamic range of the pixel values (255 for 8 bit gray scale images).

The QILV between two images x and y can be defined as

$$QILV(x, y) = \frac{2\mu_{V_x}\mu_{V_y}}{\mu_{V_x}^2 + \mu_{V_y}^2} \cdot \frac{2\sigma_{V_x}\sigma_{V_y}}{\sigma_{V_x}^2 + \sigma_{V_y}^2} \cdot \frac{\sigma_{V_xV_y}}{\sigma_{V_x}\sigma_{V_y}} \quad (21)$$

where μ_{V_x} and μ_{V_y} are the estimated means of the local variance and σ_{V_x} and σ_{V_y} are the standard deviations of the local variance respectively. $\sigma_{V_xV_y}$ is the covariance between the two images. The performance comparison of Median, NLM, and NS Median Filters based on the PSNR in dB, SSIM and QILV values for T2 Axial and T1 Sagittal slices of brain MRI corrupted with different levels of Rician noise are given in Figure 3 and Figure 4 respectively. The numerical values of the quality measures: PSNR in dB, SSIM and QILV are listed in Table 1 for the different denoising filters. As already discussed in [14], According to the values of PSNR, at High SNR (low noise level), NLM performs well than NS filter and at low SNR (high noise level), NS filter performs better than that of NLM. This result is justified by the quality measures SSIM and QILV.

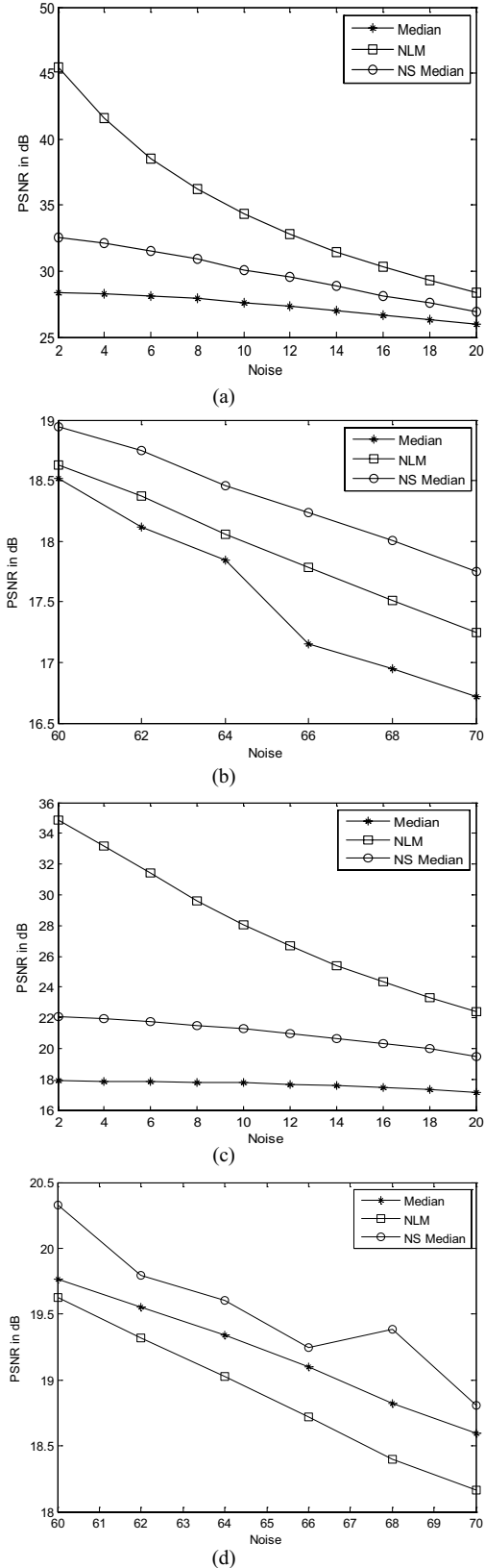


Figure 3: Comparison of Median, NLM, and NS Median Filters based on the PSNR in dB values: T2 Axial (a) High SNR (b) Low SNR; T1 Sagittal (c) High SNR (d) Low SNR.

Image	Noise	PSNR			SSIM			QILV		
		Median	NLM	NS Median	Median	NLM	NS Median	Median	NLM	NS Median
T2 Axial	2	23.18	35.65	32.69	1	1	1	0.9721	0.9947	0.9940
	10	23.14	34.36	30.41	0.8920	0.9805	0.9564	0.9048	0.9921	0.9784
	20	22.79	28.36	26.84	0.8499	0.9328	0.9096	0.8074	0.9716	0.9644
	30	22.04	24.81	24.19	0.7911	0.8644	0.8481	0.7040	0.9309	0.9226
	40	21.09	21.30	21.99	0.7199	0.7819	0.8145	0.6000	0.8685	0.8909
	50	19.94	20.27	21.05	0.6459	0.6949	0.7522	0.5109	0.7749	0.8133
	60	18.81	19.64	20.02	0.5732	0.6092	0.6961	0.4431	0.6766	0.7612
	70	17.74	18.25	19.90	0.5081	0.5336	0.6352	0.3913	0.5730	0.6879
T1 Sagittal	2	27.75	46.56	33.40	1	1	1	0.8562	0.9985	0.9970
	10	27.24	35.23	31.42	0.7537	0.9756	0.8963	0.7449	0.9883	0.9665
	20	25.89	29.19	28.14	0.7037	0.9223	0.8429	0.6384	0.9694	0.9469
	30	24.20	25.58	25.59	0.6440	0.8457	0.8244	0.5500	0.9317	0.8909
	40	22.48	22.90	23.28	0.5769	0.7586	0.7670	0.4814	0.8734	0.8593
	50	20.86	20.80	22.00	0.5149	0.6700	0.6998	0.4365	0.8038	0.8313
	60	19.44	19.07	20.36	0.4517	0.5842	0.6359	0.3984	0.7615	0.7643
	70	18.08	17.55	19.11	0.3985	0.5078	0.5795	0.3826	0.6489	0.7370

Table 1: Performance Comparison of Median, NLM and NS Median Filters

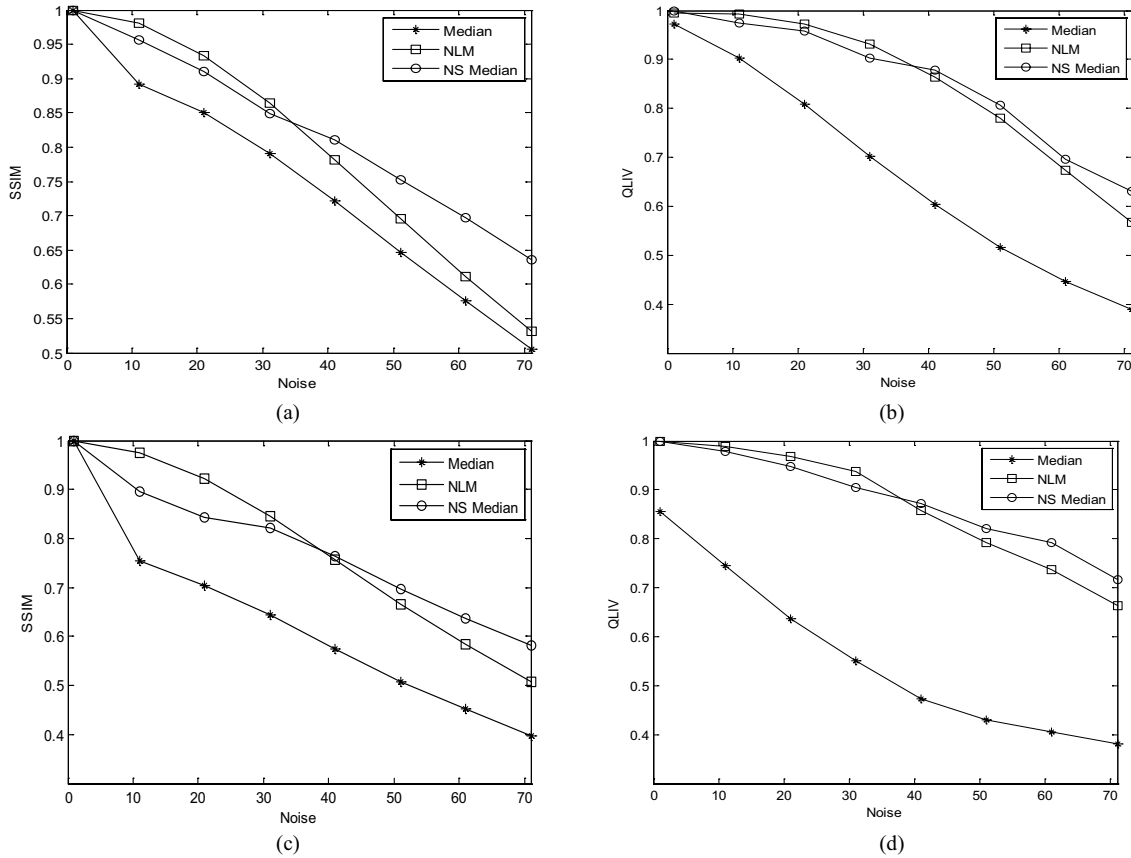


Figure 4: Comparison of Median, NLM, and NS Median Filters based on the quality measures SSIM and QILV: T2 Axial (a) SSIM (b) QILV; T1 Sagittal (c) SSIM (d) QILV.

That is, According to the structural similarity measures, by applying the Neutrosophic Set approach of median filter, the detailed structures are well preserved for low SNR compared with Median filter and Non local mean filter.

4 Conclusion

The proposed denoising technique based on Neutrosophic Set for reducing Rician noise from MR image have been validated in this article by using the structural similarity measures (SSIM, QILV). Experiments have been carried out on real MR images. This filtering method tends to produce good denoised image not only in terms of visual perception but also in terms of the quality measures such as PSNR, SSIM and QILV. This filter performs better than Median filtering method for reducing the Rician noise with different noise levels. Further, and also it outperforms the Non Local Mean approach when the noise level is high (low SNR).

References

- [1] S. Aja-Fernandez, R. San-Jose-Estepar, C. Alberola-Lopez, C.F. Westin. "Image quality assessment based on local variance". in *Proceedings 28th IEEE EMBC*, New York pp.4815-4818, (2006).
- [2] P. Bao and L. Zhang, "Noise reduction for magnetic resonance images via adaptive multiscale products thresholding," *IEEE Trans. Med. Imag.*, **22**, pp. 1089-1099, (2003).
- [3] A. Buades, B. Coll, and J. M. Morel, "A review of image denoising algorithms, with a new one," *Multiscale Modeling and Simulation*, **4**, pp. 490-530, (2005).
- [4] P. Coupe, P. Yger and C. Barillot, "Fast Non Local Means Denoising for MR Images," in *Proc. at the 9th International Conf. on Medical Image Computing and Computer assisted Intervention (MICCAI)*, Copenhagen, **4191**, pp. 33-40, (2006).
- [5] P. Coupe, P. Yger, S. Prima, P. Hellier, C. Kervrann, and C. Barillot, "An optimized blockwise nonlocal means denoising filter for 3-D magnetic resonance images," *IEEE Trans. Med. Imag.*, **27**, pp. 425-441, (2008).
- [6] I. Delakis, O. Hammad and R. I. Kitney, "Wavelet-based de-noising algorithm for images acquired with parallel magnetic resonance imaging (MRI)", *Phys. Med. Biol.*, **52**, pp. 3741-3751, (2007).
- [7] G. Gerig, O. Kubler, R. Kikinis, and F. A. Jolesz, "Nonlinear anisotropic filtering of MRI data," *IEEE Trans. Med. Imag.*, vol. 11, no. 2, pp. 221-232, Jun. 1992.
- [8] H. Gudbjartsson and S. Patz, "The Rician distribution of noisy MRI data," *Magn. Reson. Med.*, **34**, pp. 910-914, (1995).
- [9] G. Hamarneh and J. Hradsky, "Bilateral Filtering of Diffusion Tensor Magnetic Resonance Images," *IEEE Trans. Image Processing*, **16**, pp. 1723-1730, (2007).
- [10] K. Krissian and S. Aja-Fernández, "Noise driven Anisotropic Diffusion filtering of MRI", *IEEE Trans. Image Processing*, **18**, pp. 2265-2274, (2009).
- [11] J. V. Manjon, M. Robles, and N. A. Thacker, "Multispectral MRI de-noising using non-local means," *Med. Image Understand. Anal. (MIUA)*, pp. 41-46, (2007).
- [12] J. V. Manjón, J. Carbonell-Caballero, J. J. Lull, G. García-Martí, L. Martí-Bonmatí, and M. Robles, "MRI denoising using non-local means," *Med. Image Anal.*, **12**, pp. 514-523, (2008).
- [13] J. V. Manjón, P. Coupe, L. Martí-Bonmatí, D. L. Collins and M. Robles, "Adaptive Non-Local Means Denoising of MR images with spatially varying noise levels", *Magn. Reson. Imaging*, **31**, pp. 192-203, (2010).
- [14] J. Mohan, V. Krishnaveni, Yanhui Guo, "A Neutrosophic approach of MRI denoising", *Proc. IEEE International Conference on Image Information Processing*, Shimla, India, pp. 1-6, (2011).
- [15] R. D. Nowak, "Wavelet-based Rician noise removal for magnetic resonance imaging," *IEEE Trans. Image Process.*, **8**, pp. 1408-1419, (1999).
- [16] A. Pizurica, W. Philips, I. Lemahieu, and M. Acheroy, "A versatile wavelet domain noise filtration technique for medical imaging," *IEEE Trans. Med. Imag.*, **22**, pp. 323-331, (2003).
- [17] G. Placidi, M. Alecci and A. Sotgiu, "Post-processing noise removal algorithm for magnetic resonance imaging based on edge detection and wavelet analysis", *Phy. Med. Biol.*, **48**, pp. 1987-1995, (2003).
- [18] F. Samarandache, "A unifying field in logics Neutrosophic logic, in Neutrosophy. Neutrosophic Set, Neutrosophic Probability", 3rd edition, American Research Press, 2003.
- [19] J. Sijbers, A. J. den Dekker, A. Van Der Linden, M. Verhoye and D. Van Dyck, "Adaptive Anisotropic noise filtering for Magnitude MR data", *Magn. Reson. Imaging*, **17**, pp. 1533-1539, (1999).
- [20] Jinshan Tang, Qingling Sun, Jun Liu and Yongyan Cao, "An Adaptive Anisotropic Diffusion Filter for Noise Reduction in MR Images," in *Proc. IEEE International Conference on Mechatronics and Automation*, Harbin, China, pp. 1299-1304, (2007).
- [21] Z. Wang, A. C. Bovik H.R. Sheikh, E.P. Simoncell. "Image quality assessment: From error visibility to structural similarity", *IEEE Trans. Image Process*, **13**, pp. 600-612, (2004).
- [22] G. Wright, "Magnetic Resonance Imaging", *IEEE Signal Process Mag.*, **1**, pp. 56-66, (1997).
- [23] W.C.K. Wong and A.C.S. Chung, "A nonlinear and non-iterative noise reduction technique for medical images: concept and methods comparison," *Elsevier-International Congress Series*, **1268**, pp. 171-176, (2004).
- [24] W.C.K. Wong, A.C.S. Chung and S.C.H. Yu, "Trilateral filter for biomedical images", in *Proc. of ISBI*, pp- 820-823, (2004).
- [25] J. C. Wood and K. M. Johnson, "Wavelet packet denoising of magnetic resonance images: Importance of Rician noise at low SNR," *Magn. Reson. Med.*, **41**, pp. 631-635, (1999).
- [26] G. Z. Yang, P. Burger, D.N. Firmin and S. R. Underwood, "Structure Adaptive Anisotropic Filtering for Magnetic Resonance Image Enhancement", *Proceedings of CAIP*, Prague, pp.384-391, (1995).
- [27] Yanhui Guo, H. D. Cheng and Y. Zhang, "A New Neutrosophic approach to Image Denoising," *New Mathematics and Natural Computation*, **5**, pp. 653-662, (2009).
- [28] Yanhui Guo and H. D. Cheng, "New Neutrosophic approach to image segmentation," *Pattern Recognition*, **42**, pp. 587-595, (2009).
- [29] M. Zhang, L. Zhang, H. D. Cheng, "A Neutrosophic approach to image segmentation based on watershed method," *Signal Processing*, **90**, pp. 1510-1517, (2010).